Macromolecules

Article

pubs.acs.org/Macromolecules

Intrachain Folding and Interchain Association of Hyperbranched Chains with Long Uniform Subchains Made of Amphiphilic Diblock Copolymers

Lianwei Li,*[,†] Jianfeng Zhou,[‡] and Chi Wu[†,§]

[†]Hefei National Laboratory for Physical Sciences at Microscale, Department of Chemical Physics, University of Science and Technology of China, Hefei, China 230026

[‡]Research Center for Analysis and Measurement, Donghua University, Shanghai, China 201620

[§]Department of Chemistry, The Chinese University of Hong Kong, Shatin N. T., Hong Kong

ABSTRACT: Combining atom transfer radical polymerization and copper-catalyzed azide−alkyne "click" chemistry, hyperbranched copolymers with uniform poly(*tert*-butyl acrylate-*b*-styrene-*b*-*tert*-butyl acrylate) triblock copolymer subchains, denoted as hyper-(P*t*BA-PS-P*t*BA)$_n$, were successfully prepared and characterized by size exclusion chromatography (SEC), FT-IR, and ^{1}H NMR. Using laser light scattering, we first studied the intrachain contraction of ultralarge hyper-(P*t*BA$_{36}$-PS$_{55}$-P*t*BA$_{36}$)$_{600}$ chains in cyclohexane, a solvent selectively poor for PS at lower temperatures. We found that at temperatures lower than 34 °C each PS block collapses into a small globule that was stabilized by its three neighboring P*t*BA blocks with no intrachain or interchain association in a dilute solution. Further, after hydrolyzing those *tert*-butyl (*t*BA) moieties into acrylic acids (AA), we comparatively studied the interchain association of linear triblock PAA$_{23}$-PS$_{14}$-PAA$_{23}$ and its resultant hyper-(PAA$_{23}$-PS$_{14}$-PAA$_{23}$)$_n$ with different overall molar masses in water. Our results reveal that larger hyperbranched chains have a less tendency to undergo the interchain association, and the average aggregation number (N_{agg}) is scaled to the weight-average degree of polycondensation [(DP)$_w$], i.e., the number of linear triblock precursors inside each hyperbranched chain, as $N_{agg} \sim (DP)_w^{-0.7}$. As expected, increasing salt (NaCl) concentration led to stronger interchain association, resulting in large aggregates, while linear precursors only form small polymeric micelles. Moreover, our rheological study shows, unlike their linear precursor, large hyper-(PAA$_{23}$-PS$_{14}$-PAA$_{23}$)$_n$ chains can form a physical gel with a network-like structure at a concentration as low as 50 g/L, whose modulus increases with (DP)$_w$.

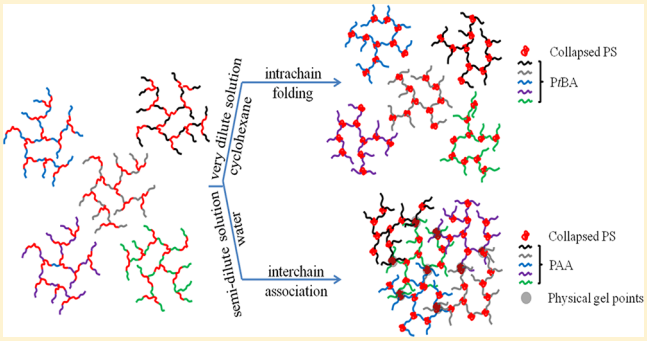

INTRODUCTION

Connecting long linear polymer chains into a hyperbranched structure leads to some unique properties in comparison with their starting linear counterparts, e.g., high toughness and good mechanical properties in bulk[1,2] and special and unique association behavior in solution,[3] to name but a few. Therefore, much effort has been spent to prepare hyperbranched polymers with different linear subchains to adjust their mechanical properties and to investigate their structure−property relationships.[1−10] However, hyperbranched chains are complicated subjects, and they are normally broadly distributed not only in their overall molar mass but also in their subchain length. In order to understand their structure−property relationships, one has to start with at least two sets of hyperbranched polymers with a precisely controlled and adjusted structure; namely, one set of chains with a similar overall molar mass (M_w) but different subchain lengths between two neighboring branching points and another set with an identical subchain length but different overall molar masses (M_w). The preparation of these well-defined hyperbranched chains has been a difficult polymer chemistry problem, hindering a quantitative study of how properties are related to chain topology. This partially explains why only few structure−property studies of long-subchain hyperbranched homopolymers with uncontrollable subchain lengths have been reported so far.[1−5] It should be mentioned that, similar to hyperbranched polymers, much efforts have been also devoted to control the subchain lengths and compositions for extremely narrowly distributed long subchain dendrimer-like polymers; however, the desired synthetic process is very tedious and time-consuming, and the subchain lengths among different generations (G) are usually not absolutely equal to each other due to the synthetic difficulty.[11−16]

Received: September 16, 2012
Revised: November 9, 2012
Published: November 16, 2012

Scheme 1. Schematic of Synthesis of Seesaw Type of Linear Triblock Copolymer (Macromonomer) and Larger Hyperbranched Amphiphilic Copolymers with Uniform Subchains, Hyper-(PAA-PS-PAA)$_n$

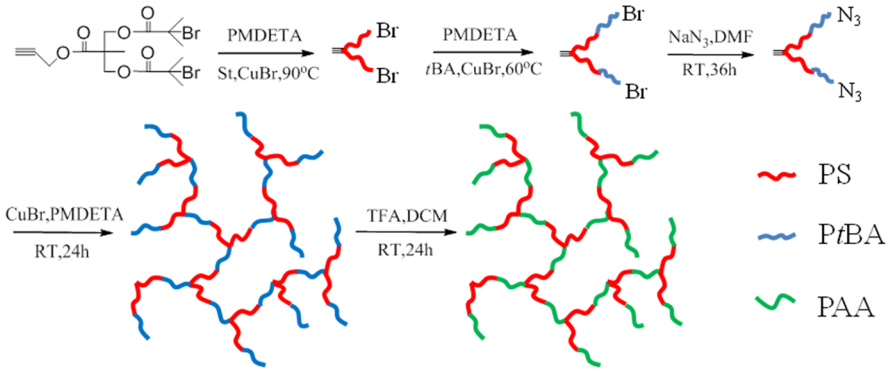

Only recently, using a specially designed seesaw-type linear macromonomer B∼∼A∼∼B (similar structure as shown in Scheme 1), where ∼∼ denotes a polystyrene (PS) chain and A and B are alkyne and azide groups, respectively, we were able to synthesize hyperbranched polymers with long and uniform polystyrene subchains.[17,18] Precipitation fractionation of such prepared hyperbranched polymers finally enables us to obtain those two sets of narrowly distributed hyperbranched polystyrenes. Armed with these hyperbranched polystyrene chains, we have experimentally established scaling laws between their molar masses (entire chain, M_w, and subchain, $M_{w,s}$) and overall chain sizes (average radius of gyration, $\langle R_g \rangle$, and average hydrodynamic radius, $\langle R_h \rangle$); determined their contracting factors (g); measured their intrinsic viscosities ($[\eta]$);[17,19] and found how they can be squeezed through a small cylindrical pore under an elongation flow with a minimal flow rate (hydrodynamic force).[20]

On the other hand, we have been interested in phase behaviors of long linear multiblock copolymer chains in a selective solvent in the past years and attempted to synthesize linear $(AB)_n$ multiblock chains with a controllable block length and sequence for investigating on the intrachain folding and interchain association.[21−23] In the current study, we extend our study further to hyperbranched chains with uniform amphiphilic diblock subchains; namely, instead of coupling uniform linear triblock chains into a long multiblock linear copolymer chain, we connect them into a well-defined hyperbranched structure. To our knowledge, there has been no theoretical or experimental study on how their phase behavior and solution properties are related to their topological structure, presumably because it is rather difficult, if not impossible, to prepare narrowly distributed hyperbranched copolymer chains with some well-defined and controllable subchain compositions.

Using the same specially designed synthetic route, instead of linear homopolymer subchain, we started to synthesize a seesaw type of linear triblock copolymer subchain, poly(*tert*-butyl acrylate)−polystyrene−poly(*tert*-butyl acrylate) (P*t*BA-PS-P*t*BA), with one alkyne group in the center of the PS block and one azide group at the end of each P*t*BA block. The narrowly distributed amphiphilic hyperbranched block copolymers, hyper-$(PAA_{23}\text{-}PS_{14}\text{-}PAA_{23})_n$, with different overall molar masses were successfully prepared by "click" chemistry, precipitation fractionation, and the *tert*-butyl group hydrolysis from *t*BA to AA, where the subscripts denote the degrees of polymerization of each block in a subchain $PAA_{23}\text{-}PS_{14}\text{-}PAA_{23}$.

Using such obtained hyperbranched amphiphilic chains and their linear triblock precursors, we investigated the conformation change of individual hyperbranched amphiphilic copolymer chains in an extremely dilute solution by using ultralarge hyperbranched block copolymer hyper-$(PtBA_{36}\text{-}PS_{55}\text{-}PtBA_{36})_n$ chains with a long PS block obtained from a preparative size excluded chromatography (SEC), where we used cyclohexane as solvent because PS changes its conformation around 34 °C and P*t*BA is always soluble in this temperature range studied. Further, we comparatively studied the interchain association and the rheological behavior of amphiphilic hyper-$(PAA_{23}\text{-}PS_{14}\text{-}PAA_{23})_n$ chains with different overall molar masses but a much short PS block as well as their initial triblock precursor in water.

EXPERIMENTAL SECTION

Materials. Styrene (St, Sinopharm, 97%) and *tert*-butyl acrylate (*t*BA, Sinopharm, 97%) was first passed through a basic alumina column to remove inhibitor and then distilled under reduced pressure over CaH_2. Copper(I) bromide (CuBr, Alfa, 98%) was washed with glacial acetic acid to remove soluble oxidized species, filtrated, washed with ethanol, and dried under vacuum. All other reagents were directly used as received.

Characterization. ^{1}H nuclear magnetic resonance (NMR) spectra were recorded on a Bruker AV400 spectrometer by using deuterated chloroform ($CDCl_3$) as solvent and tetramethylsilane (TMS) as an internal standard. The relative number- and weight-average molar masses ($M_{n,RI}$ and $M_{w,RI}$) and the absolute molar masses ($M_{w,MALLS}$ and $M_{w,MALLS}$) were determined at 35 °C by a size exclusion chromatograph (SEC, Waters 1515) equipped with three Waters Styragel columns (HR2, HR4, and HR6), a refractive index detector (RI, Wyatt WREX-02, using a conventional calibration with linear polystyrene standards), and a multiangle LLS detector (MALLS, Wyatt DAWN EOS). THF was used as an eluenting agent at a flow rate of 1.0 mL/min.

Rheological Measurements. Rheological properties were measured with a TA Instruments AR-G2 stress-controlled rheometer. A 40 mm aluminum 1° cone and a Peltier heated plate were used for the oscillatory measurements. The linear viscoelastic regime was established by an oscillatory strain sweep using different frequencies between 0.628 and 628 rad/s. Dynamic frequency sweeps were made in the linear regime at 25 °C. The measurement setup was covered with a sealing lid in order to prevent evaporation during the measurement. To prepare samples for rheological measurements, a given amount of freeze-dried hyper-$(PAA_{23}\text{-}PS_{14}\text{-}PAA_{23})$ was dissolved in distilled water directly inside a screw-capped vial at 80 °C for 10 h in a water bath. After the heating and dissolution, the solution was weighed to correct its concentration for solvent evaporation and stood at ∼25 °C for 24 h before rheological measurements.

Laser Light Scattering. A commercial LLS spectrometer (ALV/DLS/SLS-5022F) equipped with a multi-τ digital time correlator (ALV5000) and a cylindrical 22 mW UNIPHASE He−Ne laser (λ_0 = 632.8 nm) as the light source was used. In static LLS,[24,25] the angular

dx.doi.org/10.1021/ma3019415 | *Macromolecules* 2012, 45, 9391−9399

dependence of the absolute excess time-average scattering intensity, known as the Rayleigh ratio $R_{VV}(q)$, can lead to the weight-average molar mass (M_w), the root-mean-square gyration radius $\langle R_g^2\rangle_z^{1/2}$ (or simply written as $\langle R_g\rangle$) and the second virial coefficient A_2 by using

$$\frac{KC}{R_{VV}(q)} \cong \frac{1}{M_w}\left(1 + \frac{1}{3}\langle R_g^2\rangle_Z q^2\right) + 2A_2C \quad (1)$$

where $K = 4\pi^2(dn/dC)^2/(N_A\lambda_0^4)$ and $q = (4\pi/\lambda_0)\sin(\theta/2)$ with C, dn/dC, N_A, and λ_0 being concentration of the polymer solution, the specific refractive index increment, Avogadro's number, and the wavelength of light in a vacuum, respectively. The extrapolation of $R_{VV}(q)$ to $q \to 0$ and $C \to 0$ leads to M_w. The plot of $[KC/R_{VV}(q)]_{C\to 0}$ vs q^2 and $[KC/R_{VV}(q)]_{q\to 0}$ vs C lead to $\langle R_g^2\rangle_z$ and A_2, respectively. In a very dilute solution, the term of $2A_2C$ can be ignored. For our branched and ultralarge hyperbranched polymer chains, i.e., $q\langle R_g\rangle > 1$, the Berry plot is normally used. Note that our measured weight-average molar mass (M_w) is an apparent value because each copolymer chain has two comonomers with different dn/dc values. The determined dn/dc value by using a precise differential refractometer is 0.095 and 0.120 mL/g, respectively, for hyper-($PtBA_{23}$-PS_{14}-$PtBA_{23}$)$_n$ and hyper-($PtBA_{36}$-PS_{55}-$PtBA_{36}$)$_n$ in THF.

In dynamic LLS,[26] the Laplace inversion of each measured intensity−intensity time correlation function $G^{(2)}(q,t)$ in the self-beating mode can lead to a line-width distribution $G(\Gamma)$, where q is the scattering vector. For dilute solutions, Γ is related to the translational diffusion coefficient D by $(\Gamma/q^2)_{q\to 0,C\to 0} \to D$, so that $G(\Gamma)$ can be converted into a transitional diffusion coefficient distribution $G(D)$ or further a hydrodynamic radius distribution $f(R_h)$ via the Stokes−Einstein equation, $R_h = (k_BT/6\pi\eta_0)/D$, where k_B, T, and η_0 are the Boltzmann constant, the absolute temperature, and the solvent viscosity, respectively. The time correlation functions were analyzed by both the cumulants and CONTIN analysis.

Chemical Synthesis. Scheme 1 schematically shows how linear seesaw-type block copolymer macromonomers with two azide end groups and one middle alkyne group are prepared and "clicked" into large hyperbranched amphiphilic copolymer, hyper-(PAA-PS-PAA)$_n$, after hydrolyzing each tertiary butyl group into a carboxyl group. How to synthesize initiator with one alkyne and two bromine groups was described before.[17,18] Other synthesis details are outlined as follows.

Synthesis of Uniform Polystyrene Subchain via ATRP. A three-necked flask equipped with a magnetic stirring bar and three rubber septum was charged with initiator (1.0 g, 2.10 mmol), St (24 mL, 210.0 mmol), and PMDETA (435 μL, 2.1 mmol). The flask was degassed by four freeze−pump−thaw cycles and then placed in an oil bath (90 °C). After ∼2 min, CuBr (300 mg, 2.1 mmol) was introduced to start the polymerization under N_2 flow. After a few hours, the flask was cooled and diluted with THF and passed through a short column of neutral alumina to remove the metal salt. After removing all the solvents by evaporation, the residue was dissolved in THF and precipitated into an excess of methanol. After drying in a vacuum oven overnight at 40 °C, the first PS block with one alkyne and two bromine groups was obtained.

Synthesis of Uniform PtBA-PS-PtBA Triblock Subchain via ATRP. Into a three-necked flask equipped with a magnetic stirring bar and three rubber septum, linear polystyrene macroinitiator (2.8 g, 1.65 mmol), *t*BA (23.7 mL, 165 mmol), PMDETA(68.7 μL, 0.33 mmol), and acetone (5.93 mL) were charged. The flask was degassed by four freeze−pump−thaw cycles and then placed in an oil bath thermostated at 60 °C. After ∼2 min, CuBr (47.4 mg, 0.33 mmol) was introduced to start the polymerization under N_2 flow. After a few hours, the polymer mixture was cooled and diluted with THF and then passed through a short column of neutral alumina to remove the metal salt. After removing all the solvents by evaporation, the residue was dissolved in THF and precipitated into a mixture of methanol/water (3/1, v/v). After drying in a vacuum oven overnight at 40 °C, triblock P*t*BA-PS-P*t*BA with one alkyne and two bromine groups was obtained.

Azidation of Triblock Copolymer PtBA-PS-PtBA. A 100 mL round-bottom flask was first charged with triblock copolymer P*t*BA-PS-P*t*BA (7.5 g, 0.97 mmol), DMF (30 mL), and NaN_3 (0.63 g, 9.7 mmol). The mixture was allowed to stir at room temperature for 36 h. After removing most of the solvent under reduced pressure, the remaining portion was diluted with CH_2Cl_2 and then precipitated into a mixture of methanol/water (3/1, v/v). The sediments were dissolved in CH_2Cl_2 and passed through a neutral alumina column to remove the residual sodium salt and then precipitated into an excess of methanol/water (3/1, v/v). After being dried in a vacuum oven overnight at 40 °C, linear seesaw-type triblock copolymer P*t*BA-PS-P*t*BA with one alkyne and two azide groups was obtained.

Synthesis of Hyperbranched Block Copolymer Hyper-(PtBA-PS-PtBA)$_n$. A three-necked flask equipped with a magnetic stirring bar and three rubber septum was charged with P*t*BA-PS-P*t*BA macromonomer (7 g, 0.91 mmol), PMDETA (189 μL, 0.91 mmol), and DMF (35 mL). The flask was degassed by four freeze−pump−thaw cycles and then placed in a water bath thermostated at 35 °C. After ∼2 min, CuBr (131 mg, 0.91 mmol) was introduced to start the polycondensation under N_2 flow. After 24 h, the flask was rapidly cooled to room temperature. After removing most of the solvent under reduced pressure, we diluted it with THF and passed through a short column of neutral alumina to remove the metal salt. After most of the solvents are removed by a rotary evaporator, the residue was precipitated into a mixture of methanol/water (3/1, v/v). After drying in a vacuum oven overnight at 40 °C, hyperbranched block copolymer hyper-(P*t*BA-PS-P*t*BA)$_n$ was obtained.

Precipitation Fractionation. Each resultant hyper-(P*t*BA-PS-P*t*BA)$_n$ was fractionated by precipitation as follows. (1) the sample was dissolved in THF at room temperature with a concentration around 0.03 g/mL in a round-bottom flask; (2) a mixture of methanol/water (3/1, v/v) was slowly dropped in until the solution became slightly milky; (3) the temperature controlled by a water bath (±0.1 °C) was raised until the solution became clear again; (4) the solution was slowly cooled until it became slightly milky; and (5) the solution temperature was maintained to allow a very small fraction of longest chains to precipitate. Steps 2−5 were repeated to obtain a total of four fractions with different overall molar masses.

Hydrolysis of PtBA. Hyper-(P*t*BA-PS-P*t*BA)$_n$ was dissolved in dichloromethane ($C \sim 50$ g/L), and a 10-fold molar excess of trifluoroacetic acid (TFA) was added. After 24 h, TFA and dichloromethane were removed by a rotary evaporator. The collected polymer was first dissolved in 0.5 M Na_2CO_3 solution at 60 °C for 1 h, and then the solution was transferred into presoaked dialysis tubing (MWCO = 3000), dialyzed against deionized water for 5 days. The freeze-drying led to a fluffy white solid.

RESULTS AND DISCUSSION

Molecular parameters of our obtained triblock copolymers macromonomer P*t*BA-PS-P*t*BA with different St and *t*BA molar contents and molar masses are summarized in Table 1. The degrees of polymerization (DP) were calculated from area ratio of corresponding peaks in ^{1}H NMR spectrum, as shown in Figure 1.

In a typical ATRP process, the molar concentrations of CuBr−PMDETA catalyst and initiator are usually similar. However, such an equivalency leads to an uncontrollable ATRP process of *t*BA monomer. Figure 2 shows how the CuBr−

Table 1. Characterization of Linear P*t*BA-PS-P*t*BA Triblock Copolymers (Macromonomers) Prepared by ATRP

macromonomer[a]	M_n (g/mol)[b]	M_w/M_n[b]
$PtBA_{23}$-PS_{14}-$PtBA_{23}$	7.7×10^3	1.11
$PtBA_{36}$-PS_{55}-$PtBA_{36}$	1.60×10^4	1.19

[a]Degrees of polymerization (DP, subscripts are calculated from ^{1}H NMR spectra). [b]Relative number-average molar mass (M_n) and polydispersity index (M_w/M_n) are measured by size excluded chromatography using a series of linear polystyrenes as calibration standards.

dx.doi.org/10.1021/ma3019415 | Macromolecules 2012, 45, 9391−9399

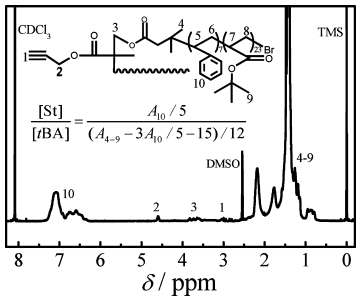

Figure 1. ^{1}H NMR spectrum of linear triblock copolymer P*t*BA$_{23}$-PS$_{14}$-P*t*BA$_{23}$ (macromonomer).

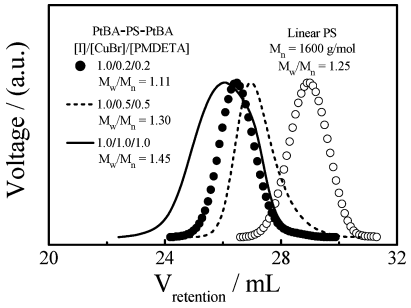

Figure 2. SEC curves of triblock copolymer P*t*BA-PS-P*t*BA with different CuBr−PMDETA catalyst concentrations.

PMDETA catalyst molar concentration affects the molar mass and polydispersity index (M_w/M_n) of the resultant triblock copolymers P*t*BA-PS-P*t*BA. Namely, M_w/M_n increases with the CuBr−PMDETA catalyst concentration, indicating the side reactions, including the outer-sphere electron transfer (OSET) induced by CuBr/CuBr$_2$[27−29] or the suppression due to the complexation between CuBr and alkyne.[27]

After decreasing the catalyst/initiator molar ratio to 1/5, we obtained narrowly distributed triblock copolymer P*t*BA-PS-P*t*BA, but the corresponding polymerization rate is low. Our results reveal that for the acrylate-derived monomers lowering the CuBr-PMDETA concentration can effectively reduce the complexation between CuBr and alkyne groups when the initiator contains an alkyne group. Therefore, linear triblock macromonomer chains used in the current study are all prepared by ATRP method with a catalyst/initiator ratio of 1/5.

Further azidation of P*t*BA-PS-P*t*BA was carried by an efficient substitution reaction of bromine groups with NaN_3 in DMF for 36 h.[28] The successful installation of two azide groups was reflected in the appearance of a N═N═N antisymmetric stretch near ∼2090 cm^{-1} upon the conversion of Br-P*t*BA-PS-P*t*BA-Br to N_3-P*t*BA-PS-P*t*BA-N_3 (Figure 3). Note that in order to directly dissolve linear triblock PAA-PS-PAA and its corresponding hyperbranched multiblock hyper-(PAA-PS-PAA)$_n$, in water without any help of an organic cosolvent, the degree of polymerization (DP) of the middle PS block should be less than 25 and its molar content should be less than 35% because styrene is strongly hydrophobic.[29,30] The addition of a cosolvent always complicates the solution behaviors because of possible preferential adsorption of one solvent on polymer chains. Therefore, to study the association and rheological behaviors of hyper-(PAA-PS-PAA)$_n$ chains in pure water, we purposefully synthesized the middle PS block with DP = 14 and a molar content of ∼23%. In addition, we heated each solution above the glass transition temperature

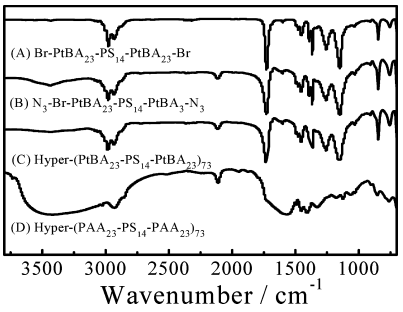

Figure 3. IR spectra of P*t*BA$_{23}$-PS$_{14}$-P*t*BA$_{23}$, where (A) before and (B) after azidation; (C) after "clicking" reaction to form hyperbranched block copolymer hyper-(P*t*BA$_{23}$-PS$_{14}$-P*t*BA$_{23}$)$_{73}$; and (D) after hydrolysis of *tert*-butyl groups to form hyperbranched block copolymer hyper-(PAA$_{23}$-PS$_{14}$-PAA$_{23}$)$_{73}$.

(T_g) of the short PS block and maintained it at 80 °C for a few hours so that its preparation history was removed. In this way, we avoided possible kinetically "frozen" interchain association. For intrachain folding study, we prepared linear P*t*BA$_{36}$-PS$_{55}$-P*t*BA$_{36}$ with a longer PS block. Instead of water, we used cyclohexane as a selective solvent because it is a good solvent for both PS and P*t*BA at temperatures higher than ∼34.5 °C but becomes a poor solvent for PS at lower temperatures.

As discussed before, the copper-catalyzed alkyne−azide cycloaddition was adopted for interchain coupling because of its high efficiency and low susceptibility to different side reactions.[23−31] Hereinafter, we use the average degree of polycondensation (DP), instead of M_n and M_w, to describe the reaction kinetics because it directly reflects how many linear triblock precursor copolymer chains are coupled into one hyperbranched chain; namely, DP is defined as $(DP)_n = M_{n,hyperbranched}/M_{n,triblock}$ or $(DP)_w = M_{w,hyperbranched}/M_{w,triblock}$. We prefer to use $(DP)_w$ because it is from the weight-average molar mass directly measured in SEC-MALLS. In order to obtain 1.0−1.5 g of narrowly distributed hyper-(P*t*BA$_{23}$-PS$_{14}$-P*t*BA$_{23}$)$_n$ fractions with different overall molar masses for rheological studies, the initial average $(DP)_w$ of resultant chains formed must be sufficiently higher with a reasonable molar mass distribution.

Figure 4 shows the obtained $(DP)_w$ increases with the initial precursor concentration, similar to our previous studies,[17,18] presumably because of a higher concentration of reactive end group and a shorter average interchain distance. Figure 4 also shows that at concentration of ∼0.35 g/mL we obtained a hyperbranched block copolymer with a high $(DP)_w \simeq 13$ and

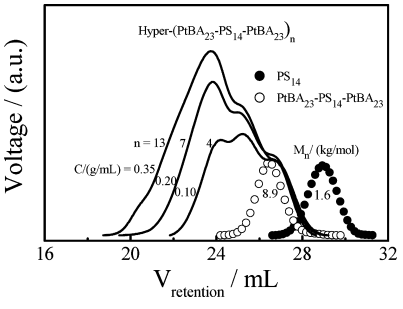

Figure 4. Initial macromonomer concentration dependence of SEC curves of resultant hyperbranched block copolymers, hyper-(P*t*BA$_{23}$-PS$_{14}$-P*t*BA$_{23}$)$_n$, after 24 h polycondensation of triblock P*t*BA$_{23}$-PS$_{14}$-P*t*BA$_{23}$ in DMF at 35 °C.

dx.doi.org/10.1021/ma3019415 | *Macromolecules* 2012, 45, 9391−9399

modest $M_w/M_n \simeq 5$, sufficiently good for further precipitation fractionation. It should be noted that further increasing the concentration is not necessary because a higher concentration will lead to a much broader molar mass distribution, while a lower concentration will decrease the overall $(DP)_w$.

Figure 5 shows four relatively narrowly distributed hyperbranched block copolymers ($M_w/M_n < 1.40$) resulted from the

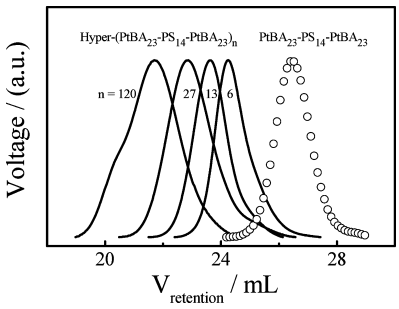

Figure 5. SEC curves of four fractions of hyperbranched block copolymer hyper-($PtBA_{23}$-PS_{14}-$PtBA_{23}$)$_n$ with different overall molar masses, which were obtained by precipitation fractionation.

precipitation fractionation. The ^{1}H NMR and UV spectra (not shown) revealed that their styrene contents are nearly identical. After coupling linear triblock copolymer chains together, the intensity related to the azide stretching still partially remains (Figure 3C) because only no more than half of the azide end groups are consumed in the "clicking" reaction. The deprotection of *tert*-butyl groups is reflected in the broad carboxylic-OH stretching peak (~3700−2600 cm^{-1}) and the shifting of the carbonyl stretching peak (~1730 cm^{-1}) to a lower wavenumber, as shown in Figure 3D, indicating that the hydrolysis of *tert*-butyl groups is nearly complete.[34] The broadening of the carbonyl stretching peak can be attributed to the presence of both free carboxylic acid and hydrogen-bonding formation groups.[35] Note that many previous experiments have revealed that the ester bonds in the chain backbone undergo no cleavage during the TFA deprotection step,[36] so that further characterization of the resultant copolymers after the deprotection is not necessary.

These fractions of hyper-(PAA_{23}-PS_{14}-PAA_{23})$_n$ were used to study the interchain association and rheological behaviors of amphiphilic hyperbranched block copolymers in water. It should be noted that for the intrachain folding study ultralarge hyperbranched chain hyper-($PtBA_{36}$-PS_{55}-$PtBA_{36}$)$_{600}$ with a narrow molar mass distribution was directly prepared by a preparative SEC instead of the precipitation fractionation because here we only need a very small amount of sample (10^2 μg).

Previously, it was predicted that the folding and contraction of linear $(AB)_n$ multiblock copolymer chains in a selective solvent could result in single-chain micelles or a string of small micelles on the chain backbone, depending on the lengths of the A and B blocks as well as on the overall chain length.[37] The current hyperbranched structure makes things much more complicated than linear counterpart. In order to study intrachain folding of individual chains, we used a preparative SEC to get a narrowly distributed hyper-($PtBA_{36}$-PS_{55}-$PtBA_{36}$)$_{600}$ with $M_w/M_n \sim 1.15$, as shown in Figure 6. Note that M_w from the RI detector is about 3 times smaller than that from the MALLS detector. This is because the scattered light intensity is proportional to the square of the mass of a

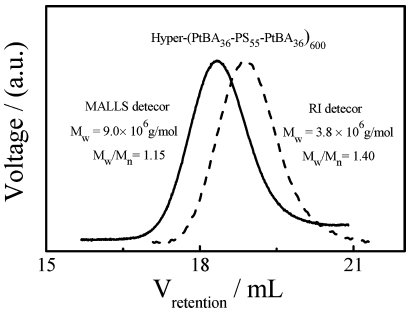

Figure 6. SEC curves of hyper-($PtBA_{36}$-PS_{55}-$PtBA_{36}$)$_{600}$ with two different detectors: RI (dashed line) and MALLS (solid line).

scattering object, i.e., one larger hyperbranched copolymer chain weights many times more than smaller ones in light scattering. In addition, the branching effect will also result in a deviation of the real molar mass (MALLS detector) from the apparent one (RI detector). Hereafter, we will only use the results from LLS.

We further used a combination of static and dynamic LLS to characterize this narrowly distributed hyper-($PtBA_{36}$-PS_{55}-$PtBA_{36}$)$_{600}$ fraction in a good solvent (THF) and a selective solvent (cyclohexane). For comparison, we also studied a hyperbranched PS homopolymer, hyper-(PS_{700})$_{120}$. In our case, the Zimm plot with a workable size range of 20−50 nm did not yield a linear plot so that we have alternatively used the Berry plot; i.e., we plotted $[KC/R_{VV}(q)]^{1/2}$ versus $(q^2 + kC)$, which is better for us to extract M_w and $\langle R_g \rangle$, as shown in Figure 7,

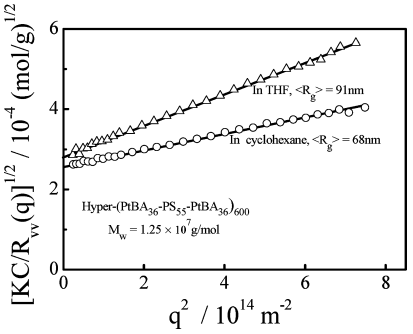

Figure 7. Angular dependence of $[KC/R_{VV}(q)]^{1/2}$ (the Berry plot) of hyper-($PtBA_{36}$-PS_{55}-$PtBA_{36}$)$_{600}$ in THF, good for both P*t*BA and PS blocks, and in cyclohexane, only selectively good from P*t*BA block.

where we ignored the concentration correction because the solution is so dilute ($C \sim 10^{-5}$ g/mL). The decrease of $\langle R_g \rangle$ clearly shows the contraction of hyper-($PtBA_{36}$-PS_{55}-$PtBA_{36}$)$_{600}$ chains in cyclohexane. On the other hand, the extrapolation to the zero scattering angle ($q \rightarrow 0$) leads to a similar intercept, indicating that no interchain association occurs in cyclohexane. The smaller size in cyclohexane reflects that for polystyrene the solvent quality of THF is much better than cyclohexane at 25 °C.

Figure 8 shows that $\langle R_h \rangle$ decreases from 76.0 to 57.5 nm, directly revealing the intrachain contraction of individual PS blocks in a hyperbranched chain in cyclohexane as the solution is cooled down. Both $\langle R_g \rangle$ and $\langle R_h \rangle$ of the hyperbranched chains in cyclohexane are smaller than that in THF because of the shrinking of the PS blocks in cyclohexane. It is interesting to note that the ratios of $\langle R_g \rangle/\langle R_h \rangle$ in two solvents nearly remain a constant value of ~1.2, a typical value for

dx.doi.org/10.1021/ma3019415 | *Macromolecules* 2012, 45, 9391−9399

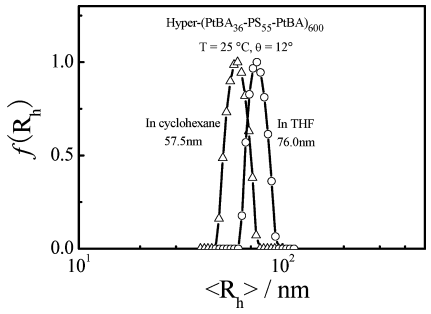

Figure 8. Hydrodynamic radius distributions of hyperbranched hyper-$(PtBA_{36}\text{-}PS_{55}\text{-}PtBA_{36})_{600}$ in THF, good for both P*t*BA and PS blocks, and in cyclohexane, only selectively good from P*t*BA block.

hyperbranched chains, revealing that hyperbranched chains have a very similar chain conformation in these two solvents even the PS blocks slightly shrink in cyclohexane.

Figure 9 shows that lowering the solution temperature from 60 to 10 °C has nearly no effect on M_w of hyperbranched

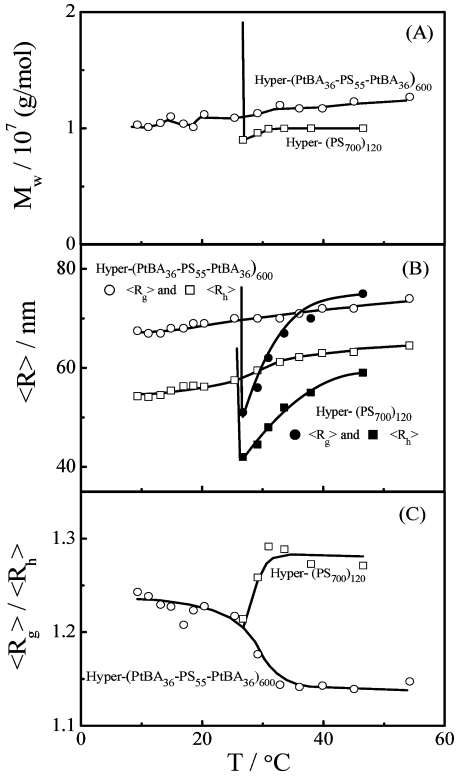

Figure 9. Temperature dependences of (A) weight-average molar mass (M_w), (B) average radius of gyration ($\langle R_g \rangle$) and average hydrodynamic radius ($\langle R_h \rangle$), and (C) $\langle R_g \rangle/\langle R_h \rangle$ of hyper-$(PtBA_{36}\text{-}PS_{55}\text{-}PtBA_{36})_{600}$ copolymer and hyper-$(PS_{700})_{120}$ homopolymer in cyclohexane, a solvent selectively poor for PS blocks at temperatures lower than ~34.5 °C.

copolymer chains but leads to a very sharp increase of M_w of hyperbranched homopolymer chains at ~28 °C, signaling the interchain association, which is expected because unlike the copolymer chains there is no soluble P*t*BA blocks to stabilize those collapsed PS subchains and prevent them to phase out of the solution. Such intrachain contraction and interchain association are also directly reflected in the decrease of both $\langle R_g \rangle$ and $\langle R_h \rangle$. It is also understandable that the hyperbranched homopolymer chains shrink much more than their copolymer counterparts. It should be stated that the time-average scattering intensity of the copolymer solution after the extrapolation to the zero scattering angle remains a constant in the temperature range 10−60 °C (not shown), also indicating that no interchain association occurred even at ~10 °C, at which cyclohexane is a very poor solvent for PS.

Figure 9C shows that for the hyperbranched homopolymer $\langle R_g \rangle/\langle R_h \rangle$ decreases as the temperature decreases before the chains start to associate because $\langle R_g \rangle$ decreases faster than $\langle R_h \rangle$. Note that $\langle R_g \rangle$ describes how mass is distributed in space, while $\langle R_h \rangle$ contains the hydrodynamic draining. Such a size decrease as the chain shrinks was also observed for linear homopolymer chains before because of a less change in $\langle R_h \rangle$,[38−40] especially in the low temperature region. However, an opposite trend was observed for the hyperbranched copolymer chains, presumably because the shrinking of each PS block makes the subchain less flexible, which has an opposite effect on $\langle R_g \rangle$.

Here the formation of a single-flower conformation is unlikely because each collapsed PS block is hindered by three soluble P*t*BA blocks that are linked to other triblock subchains. The occurrence of intrachain contraction with no interchain association in a very dilute solution is mainly attributed to the existence of those soluble P*t*BA blocks on its periphery. Scheme 2 schematically shows how a large hyperbranched block copolymer chain changes its chain conformation in a solvent selectively poor for the middle block.

Scheme 2. Schematic of How a Hyper-$(PtBA_{36}\text{-}PS_{55}\text{-}PtBA_{36})_{600}$ Chain Changes Its Conformation in Cyclohexane at Lower Temperatures

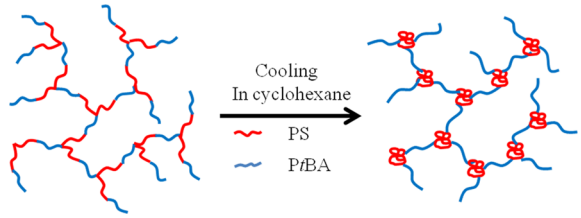

Before using LLS to study interchain association of hyperbranched block copolymer chains in aqueous solutions, we first determined their differential refractive index increments (d*n*/dC) of hyper-$(PAA_{23}\text{-}PS_{14}\text{-}PAA_{23})_n$ in 0.1 and 1.0 M NaCl aqueous solution, which are 0.17 and 0.19 mL/g, respectively, slightly larger than the reported values in the literature.[41] The addition of NaCl is to suppress the polyelectrolytes effect. It should be stated that for all the solutions, pH ~ 9.0. This is because the AA group used was in the sodium salt form (−COONa) and most of the −COONa groups (~95%) are ionized into $-COO^-$ and Na^+ in water according to the literature.[42,43]

Figure 10 shows that larger hyperbranched block copolymer chains have a less tendency to undergo interchain association and the average aggregation number (N_{agg}) is related to the weight-average degree of polycondensation ($(DP)_w$) as $N_{agg} \sim (DP)_w^{-0.7}$, where N_{agg} was defined as the molar mass ratio of aggregates and triblock precursor, i.e., $M_{w,agg}/M_{w,triblock}$. Presumably, in a large hyper-$(PAA_{23}\text{-}PS_{14}\text{-}PAA_{23})_n$ chain, most of its hydrophobic PS blocks are inevitably wrapped, protected, and stabilized by those hydrophilic PAA blocks at its periphery so that the interchain association is hindered, resulting in a smaller N_{agg}.

dx.doi.org/10.1021/ma3019415 | *Macromolecules* 2012, 45, 9391−9399

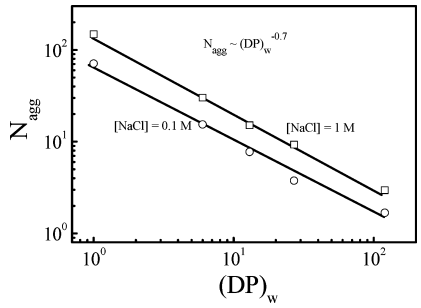

Figure 10. Degree of polycondensation $(DP)_w$ dependence of average aggregation number (N_{agg}) of hyper-$(PAA_{23}$-PS_{14}-$PAA_{23})_n$ chains in different aqueous solutions, where $C_{copolymer}$ = 1.0 g/L.

Figure 11 reveals that adding salt promotes the interchain association of hyperbranched chains in spite of their different

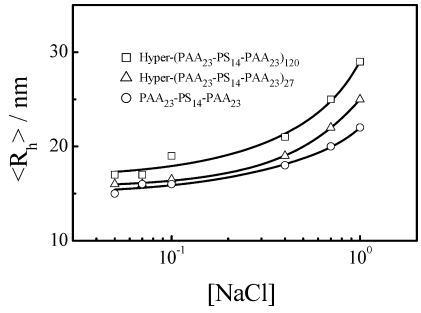

Figure 11. Salt concentration dependence of average hydrodynamic radius ($\langle R_h \rangle$) of hyper-$(PAA_{23}$-PS_{14}-$PAA_{23})_n$ and their corresponding linear triblock precursor PAA_{23}-PS_{14}-PAA_{23}.

initial sizes, but for a given salt concentration, the increment of the average hydrodynamic size of the resultant aggregates increases with its initial size, i.e., $(DP)_w$, which is expected. It should be noted that the addition of salt into the solution makes the PAA block contract and reduces its stabilization role (promotes the interchain association, as shown in Figure 10). The intrachain contraction and interchain association have opposite effects on $\langle R_h \rangle$. The results in Figure 11 indicate that the interchain association overrides the intrachain contraction of the PAA blocks. It is worth noting that in the high salt range 0.1−1.0 M linear triblock precursor can only form more compacted micelle-like aggregates via the hydrophobic association of those collapsed PS blocks. In contrast, the interchain association of those collapsed PS blocks among different hyperbranched chains is more difficult because most of them are entrapped inside and surrounded by soluble hydrophilic PAA blocks. Therefore, the interchain association of hyperbranched chains only occurs via those collapsed PS blocks near their periphery, resulting in a loosely connected microgel-like structure with a larger $\langle R_h \rangle$, as shown in Scheme 3. As expected, if the copolymer concentration is higher than the overlapping concentration (C^*), i.e., in the semidilute regime, the interchain association of those collapsed PS blocks will act as physical cross-linking points to form a gel-like structure that can be better examined by rheological measurements.

Figure 12A shows that the storage modulus (G') of hyper-$(PAA_{23}$-PS_{14}-$PAA_{23})_6$ chains in aqueous solution gradually increases with its concentration (C) and finally exceeds its loss modulus (G'') at $C \sim 50$ g/L, revealing a gel-like behavior.

Scheme 3. Schematic of How Hyper-$(PAA_{23}$-PS_{14}-$PAA_{23})_n$ Chains Undergo Interchain Association to Form a Gel-like Network, Where PAA Blocks from Different Chains Are Represented by Different Colors

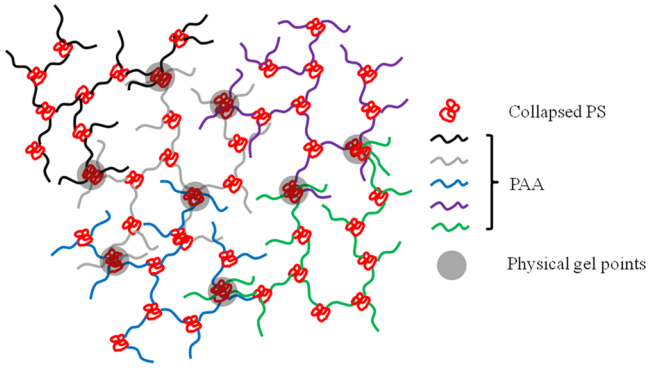

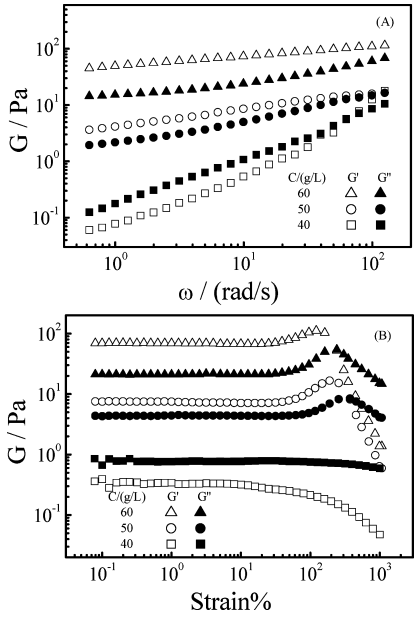

Figure 12. (A) Oscillatory frequency and (B) strain dependence of hyper-$(PAA_{23}$-PS_{14}-$PAA_{23})_6$ aqueous solutions with different copolymer concentrations.

Further increase of C to 60 g/L led to a free-standing gel. Figure 12B shows a strain-hardening feature, typical for solutions containing associative polymers; namely, G' increases with strain after an initial flat regime but before the shear thinning occurs at higher strains. As expected, no gel-like behavior was observed for triblock PAA-PS-PAA precursor even when C reached 200 g/L.

Figure 13 shows that for a given copolymer concentration both G' and G'' increase with $(DP)_w$. Theoretically, for a space (V) containing N uniform hard spheres with a radius of R without any specific interaction, their volume fraction (ϕ_{sphere}) can be expressed as $\phi_{sphere} = (4\pi R^3/3)N/V = C/C^*$. Assuming each hyperbranched chain as a sphere and using the scaling law $R_g \sim M_w^{1/2}$ for ideal hyperbranched chains, we have

$$C^* = \frac{M_W}{(4\pi R_g^{\,3}/3)N_A} \sim M_W^{-1/2} \quad (2)$$

Therefore, for a given weight/volume concentration (C), larger hyper-$(PAA_{23}$-PS_{14}-$PAA_{23})_n$ chains have a higher volume

dx.doi.org/10.1021/ma3019415 | Macromolecules 2012, 45, 9391−9399

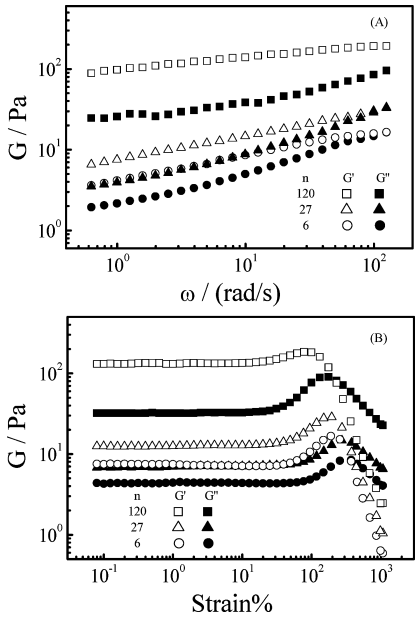

Figure 13. (A) Oscillatory frequency and (B) strain dependence of hyper-$(PAA_{23}\text{-}PS_{14}\text{-}PAA_{23})_n$ aqueous solutions with different degrees of polycondensation $(DP)_w$, where C = 50 g/L.

fraction, leading to a higher modulus. However, a quantitative description between the volume fraction and the modulus is rather difficult because of several reasons: (1) we need the prefactor in the scaling law $R_g \sim M_w^{1/2}$; (2) each hyperbranched chain is not a hard sphere; and (3) the modulus of our gel-like system is related to both the interchain hydrophobic interaction among those collapsed PS blocks and the interchain entanglements among the swollen PAA blocks on periphery.

CONCLUSION

In order to obtain seesaw-type linear poly(*tert*-butyl acrylate-*b*-styrene-*b*-*tert*-butyl acrylate) triblock copolymer precursors (P*t*BA-PS-P*t*BA), the optimal ATRP catalyst/initiator ratio (1/5) should be used. Clicking these linear precursors together by the azide−alkyne reaction results in large hyperbranched block copolymers, hyper-$(PtBA\text{-}PS\text{-}PtBA)_n$ with uniform subchains. The fractionation of each resultant hyper-$(PtBA\text{-}PS\text{-}PtBA)_n$ by a preparative size excluded chromatography or by precipitation can lead to a set of narrowly distributed hyperbranched chains with different overall molar masses but an identical subchain length. We found large hyper-$(PtBA_{36}\text{-}PS_{55}\text{-}PtBA_{36})_{600}$ chains undergo intrachain folding in a solvent (cyclohexane) selectively poor for PS at lower temperatures; namely, each PS block collapses into a small globule stabilized by its three neighboring soluble P*t*BA blocks without any intrachain or intrachain association. The hydrolysis of each *tert*-butyl (*t*BA) moiety into an acrylic acid (AA) leads to hyper-$(PAA_{23}\text{-}PS_{14}\text{-}PAA_{23})_n$ chains that associate with each other in water but large hyper-$(PAA_{23}\text{-}PS_{14}\text{-}PAA_{23})_n$ chains tend to undergo the intrachain folding instead of the interchain association. The average aggregation number (N_{agg}) is roughly scaled to the weight-average degree of polycondensation ($(DP)_w$) as $N_{agg} \sim (DP)_w^{-0.7}$. Increasing the salt (NaCl) concentration results in stronger interchain association of hyper-$(PAA_{23}\text{-}PS_{14}\text{-}PAA_{23})_n$ while their linear triblock precursor only forms small micelle-like interchain aggregates. As expected, increasing the concentration of hyper-$(PAA_{23}\text{-}PS_{14}\text{-}PAA_{23})_n$ to 50 g/L can result in a physical gel. The increase of modulus of such a gel network with $(DP)_w$ can be attributed to the fact that for a given weight concentration larger hyperbranched chains occupy a higher volume fraction inside a solution. The current study has showed how the chain topology affects the solution properties and provided useful data for further theoretical modeling.

AUTHOR INFORMATION

Corresponding Author

*E-mail: llw@mail.ustc.edu.cn.

Notes

The authors declare no competing financial interest.

ACKNOWLEDGMENTS

The financial support of The National Natural Science Foundation of China Projects (20934005 and 51173177), The Ministry of Science and Technology Key Project (2012CB933802), and The Hong Kong SAR Earmarked Projects (CUHK4042/10P, 2130241; CUHK4036/11P, 2130281 and 2060431) is gratefully acknowledged.

REFERENCES

(1) Hutchings, L.; Dodds, J.; Rees, D.; Kimani, S.; Wu, J.; Smith, E. *Macromolecules* **2009**, *42*, 8675.
(2) Clarke, N.; Luca, E. D.; Dodds, J. M.; Kimani, S. M.; Hutchings, L. R. *Eur. Polym. J.* **2008**, *44*, 665.
(3) Konkolewicz, D.; Poon, C.; Gray-Weale, A.; Perrier, S. *Chem. Commun.* **2010**, *47*, 239.
(4) Hutchings, L. R.; Dodds, J. M.; Roberts-Bleming, S. J. *Macromolecules* **2005**, *38*, 5970.
(5) Dodds, J. M.; De Luca, E.; Hutchings, L. R.; Clarke, N. *J. Polym. Sci., Part B: Polym. Phys.* **2007**, *45*, 2762.
(6) Konkolewicz, D.; Monteiro, M. J.; Perrier, S. b. *Macromolecules* **2011**, *44*, 7067.
(7) Konkolewicz, D.; Gray-Weale, A.; Perrier, S. *J. Am. Chem. Soc.* **2009**, *131*, 18075.
(8) Hutchings, L.; Dodds, J.; Roberts-Bleming, S. *Macromol. Symp.* **2006**, *240*, 56.
(9) Trollsås, M.; Hedrick, J. L. *Macromolecules* **1998**, *31*, 4390.
(10) Unal, S.; Yilgor, I.; Yilgor, E.; Sheth, J. P.; Wilkes, G.; Long, T. *Macromolecules* **2004**, *37*, 7081.
(11) Feng, X.; Taton, D.; Chaikof, E. L.; Gnanou, Y. *Macromolecules* **2009**, *42*, 7292.
(12) Feng, X.; Taton, D.; Ibarboure, E.; Chaikof, E. L.; Gnanou, Y. *J. Am. Chem. Soc.* **2008**, *130*, 11662.
(13) Sun, W.; He, J.; Wang, X.; Zhang, C.; Zhang, H.; Yang, Y. *Macromolecules* **2009**, *42*, 7309.
(14) Yoo, H.-S.; Watanabe, T.; Hirao, A. *Macromolecules* **2009**, *42*, 4558.
(15) Yoo, H.-S.; Watanabe, T.; Matsunaga, Y.; Hirao, A. *Macromolecules* **2011**, *45*, 100.
(16) Zhang, H.; He, J.; Zhang, C.; Ju, Z.; Li, J.; Yang, Y. *Macromolecules* **2011**, *45*, 828.
(17) Li, L.; He, C.; He, W.; Wu, C. *Macromolecules* **2011**, *44*, 8195.
(18) He, C.; Li, L.; He, W.; Jiang, W.; Wu, C. *Macromolecules* **2011**, *44*, 6233.
(19) Li, L.; Lu, Y.; An, Li.; Wu, C. To be submitted to *Macromolecules*.
(20) Li, L.; He, C.; He, W.; Wu, C. *Macromolecules* **2012**, *45*, 7583.
(21) Zhang, G.; Wu, C. *Adv. Polym. Sci.* **2006**, *195*, 101.
(22) Zhang, Q.; Ye, J.; Lu, Y.; Nie, T.; Xie, D.; Song, Q.; Chen, H.; Zhang, G.; Tang, Y.; Wu, C.; Xie, Z. *Macromolecules* **2008**, *41*, 2228.
(23) Hong, L.; Zhu, F.; Li, J.; Ngai, T.; Xie, Z.; Wu, C. *Macromolecules* **2008**, *41*, 2219.

(24) Zimm, B. H. *J. Chem. Phys.* **1948**, *16*, 1099.
(25) Chu, B. *Laser Scattering*, 2nd ed.; Academic Press: New York, 1991.
(26) Berne, B.; Pecroa, R. *Dynamic Light Scattering*; Plenum Press: New York, 1976.
(27) Chen, F.; Liu, G.; Zhang, G. *J. Polym. Sci., Polym. Chem.* **2011**, *50*, 831.
(28) Laurent, B. A.; Grayson, S. M. *J. Am. Chem. Soc.* **2006**, *128*, 4238.
(29) Hietala, S.; Strandman, S.; Järvi, P.; Torkkeli, M.; Jankova, K.; Hvilsted, S.; Tenhu, H. *Macromolecules* **2009**, *42*, 1726.
(30) Hietala, S.; Mononen, P.; Strandman, S.; Järvi, P.; Torkkeli, M.; Jankova, K.; Hvilsted, S.; Tenhu, H. *Polymer* **2007**, *48*, 4087.
(31) Binder, W. H.; Sachsenhofer, R. *Macromol. Rapid Commun.* **2007**, *28*, 15.
(32) Binder, W. H.; Sachsenhofer, R. *Macromol. Rapid Commun.* **2008**, *29*, 952.
(33) Bock, V. D.; Hiemstra, H.; van Maarseveen, J. H. *Eur. J. Org. Chem.* **2006**, 51.
(34) Wang, G.; Tong, X.; Zhao, Y. *Macromolecules* **2004**, *37*, 8911.
(35) Motzer, H. R.; Painter, P. C.; Coleman, M. M. *Macromolecules* **2001**, *34*, 8390.
(36) Pang, X.; Zhao, L.; Akinc, M.; Kim, J. K.; Lin, Z. *Macromolecules* **2011**, *44*, 3746.
(37) Halperin, A. *Macromolecules* **1991**, *24*, 1418.
(38) Wu, C.; Zhou, S. *Macromolecules* **1995**, *28*, 5388.
(39) Wu, C.; Zhou, S. *Macromolecules* **1995**, *28*, 8381.
(40) Wu, C.; Wang, X. *Phys. Rev. Lett.* **1998**, *80*, 4092.
(41) Burguière, C.; Chassenieux, C.; Charleux, B. *Polymer* **2003**, *44*, 509.
(42) Colombani, O.; Ruppel, M.; Schubert, F.; Zettl, H.; Pergushov, D.; Müller, A. *Macromolecules* **2007**, *40*, 4338.
(43) Colombani, O.; Ruppel, M.; Burkhardt, M.; Drechsler, M.; Schumacher, M.; Gradzielski, M.; Schweins, R.; Müller, A. *Macromolecules* **2007**, *40*, 4351.